Disclaimer

Version history:

Version 1: 2021/07/28: Submitted to EarthArXiv

The impact of spatially varying ice sheet basal conditions on sliding at glacial time scales

Evan J. GOWAN,[1,2,*] Sebastian HINCK,[1] Lu NIU,[1] Caroline CLASON,[3] Gerrit LOHMANN[1,2]

[1]*Alfred-Wegener-Institut Helmholtz-Zentrum für Polar- und Meeresforschung, Bremerhaven, Germany*

[2]*MARUM, University of Bremen, Bremen, Germany*

[3]*School of Geography, Earth and Environmental Sciences, University of Plymouth, Plymouth, United Kingdom*

[*] *now at Faculty of Advanced Science and Technology, Kumamoto University, Kumamoto, Japan*

Correspondence: Evan J. Gowan <evangowan@gmail.com>

ABSTRACT. Spatially variable bed conditions govern how ice sheets behave at glacial time scales (>1000 years). The presence or lack of complete sediment cover is responsible for changes in dynamics between the core and peripheral regions of the Laurentide and Fennoscandian ice sheets. A key component of this change is because sliding is promoted when unconsolidated sediments below the ice become water saturated, and become weaker than the overlying ice. We present an ice sheet sliding module for the Parallel Ice Sheet Model (PISM) that takes into account changes in sediment cover. This model routes meltwater, derived from the surface and base of the ice sheet, towards the margin of the ice sheet. The sliding is accomplished through water saturated sediments, or through hard-bedded sliding induced by changes in the effective pressure in the water drainage system. In areas with continuous, water saturated sediments, sliding is almost always accomplished through sediment deformation, except during times of high discharge. In areas with even a small portion of bare rock, sliding is dependent on the seasonally changing supply

of water. Our model causes a more rapid buildup of ice sheets compared to a sediment-deformation only model, especially into areas with complete sediment cover.

INTRODUCTION

Proper parameterization of the basal boundary condition of ice sheets is essential to evaluate their history, and to project how they will behave in the future. For contemporary ice sheets, it is possible to make a general inference on basal properties based on present day observations of velocity, bed topography and ice surface height (*e.g.* Joughin and others, 2004; Shapero and others, 2016), or through geophysical measurements (*e.g.* Anandakrishnan and Winberry, 2004; Walter and others, 2014). The velocity of glaciers is influenced by seasonal variations in water reaching the base, which causes acceleration during the melt season (Zwally and others, 2002; van de Wal and others, 2008). An ice sheet model should be able to incorporate the presence of deforming sediments (Alley and others, 1986) and hydrologically induced velocity changes (Clason and others, 2015).

Most actively developed ice sheet models incorporate a basal sliding law using the shallow shelf approximation and the hypothesis that the bed is covered by deformable sediments (for instance PISM Bueler and Brown (2009); Winkelmann and others (2011); PISM authors (2017)), or a spatially varying basal traction constant in a Coulomb friction and/or power law sliding (for instance, BISICLES (Cornford and others, 2013), SICOPOLIS (Bernales and others, 2017) Elmer/Ice (Gagliardini and others, 2007), ISSM (Morlighem and others, 2010), and Community Ice Sheet Model (CISM) (Lipscomb and others, 2019)). These models were generally developed for use within the existing Greenland and Antarctic ice sheets, where details on the nature of basal conditions are limited. Earlier ice sheet models using simpler ice flow approximations demonstrated the importance of hydrology on ice sheet evolution (Arnold and Sharp, 2002; Clason and others, 2014). At present, there is no open source ice sheet model that couples seasonally changing hydrological conditions, and basal conditions that include changes in sediment cover, while using the more advanced ice flow physics. For the North American and Eurasian ice sheets, although we know about the distribution of sediments and can make inferences on ice sheet flow based on landforms (Stokes and Clark, 2001; Margold and others, 2015; Greenwood and others, 2017), the constants used in the sliding laws used in ice sheet models have no reference ice thickness or velocity field in which to tune them. Therefore, it is desirable to create a more sophisticated sliding law that can utilize observations from surficial geology and geomorphology.

We present a new basal condition model within the Parallel Ice Sheet Model 1.0 (PISM) (Bueler and Brown, 2009; Winkelmann and others, 2011; PISM authors, 2017) that incorporates these features. Our intent is to create a model that provides more realistic basal boundary conditions, while still being efficient enough to run on glacial time scales. Our model is computationally inexpensive, even over a continental size domain, and is therefore suitable for simulating paleo ice sheets. We provide a suite of tests of the variables available within the model, and provide recommendations on usage. Finally, we apply the model to the North American continent to simulate the Cordillera and Laurentide ice sheets, to show how the change in basal conditions affected ice sheet growth and retreat.

METHODS

Hydrology model

The hydrology model is based on the concept that a certain amount of water gets stored in the sediments underlying the ice sheets, and, once saturated, the excess is transported in the direction of the hydrological gradient to the ice margin. Some components of our model derive from the routing scheme described by Bueler and van Pelt (2015), but we have simplified the implementation to emphasize computation speed. Our model does not conserve mass, and instantly transports water to the edge of the ice sheet. The water from upstream is added to each grid cell downstream. This is not entirely realistic, but since the time stepping in the model is usually on the order of days to months, while hydrologically induced acceleration of glaciers can happen on the order of hours (Bartholomew and others, 2012), it can be considered to be representative of average conditions. Ultimately, the output of the hydrology model is the effective pressure at the base of the ice sheet, which is then fed into the basal sliding model. A schematic of the components of our model is shown on Fig. 1, while Fig. 2 shows the workflow of the model.

Water routing

The first component of the model is that it captures the surface melt. We are using the semi-analytical positive degree day (PDD) method module (Calov and Greve, 2005). As implemented in PISM, it computes the amount of ice that melts at the surface as a diagnostic parameter. Our modification stores this value and passes it to our hydrology model. Within our model, there is an option to set the fraction of the meltwater that gets transfered to the base of the ice sheet (see Table 1 for a full list of command line options available

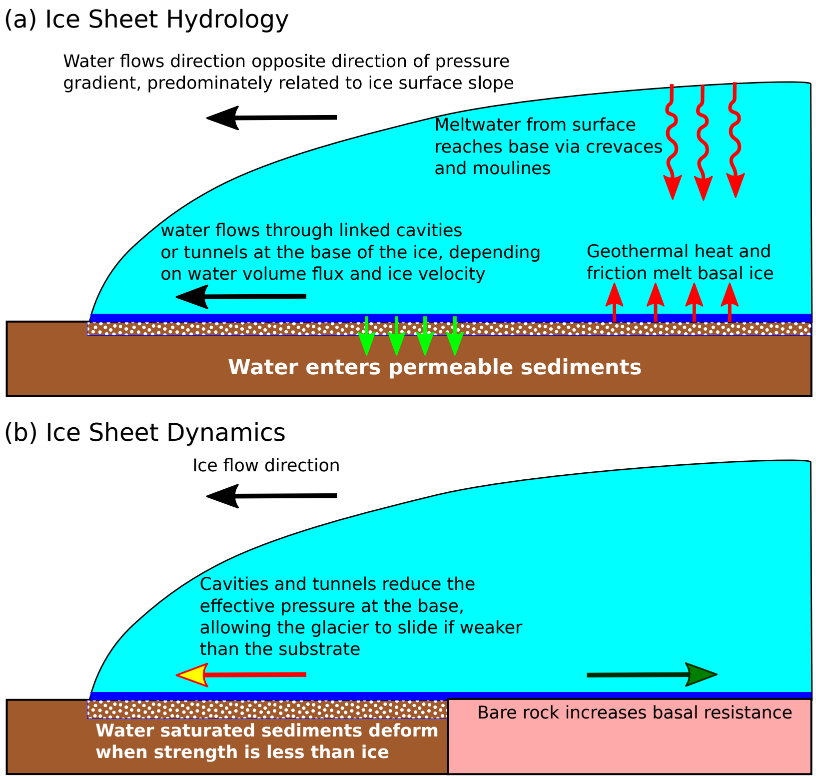

Fig. 1. Schematic of the components of the new basal conditions model. (a) Overview of ice sheet hydrology. (b) Overview of impact on sliding.

for the model). The water transfered from the surface is added to the meltwater generated from heating at the base (Aschwanden and others, 2012). After this, the water is automatically routed towards the edge of the ice sheet in the direction of the potential gradient.

The next step is a modification of the undrained plastic bed model (Tulaczyk and others, 2000; Bueler and Brown, 2009). In this model, a layer of sediment of a specified thickness and porosity fills with water until it is saturated, which is set within PISM as a "water thickness" parameter (which we set to be a maximum 1 m, as in Niu and others (2019b)). A certain percentage of accumulated water is allowed to disperse at every time step in order to simulate drainage. At every grid cell, if the water thickness is less than the maximum value, any subglacial water will be added to the sediments. Our modification from the default model is that the amount of water that can enter the subsurface depends on the fraction of the surface that is covered in sediment. If the sediment cover is incomplete, then the sediments can fill with water to the maximum level faster than if there is complete cover since there is less sediment to accommodate the water. Note that our model does not take into account the possibility that the underlying sediments are impenetrable due to being frozen. Any excess water after filling the sediments is passed to the next step.

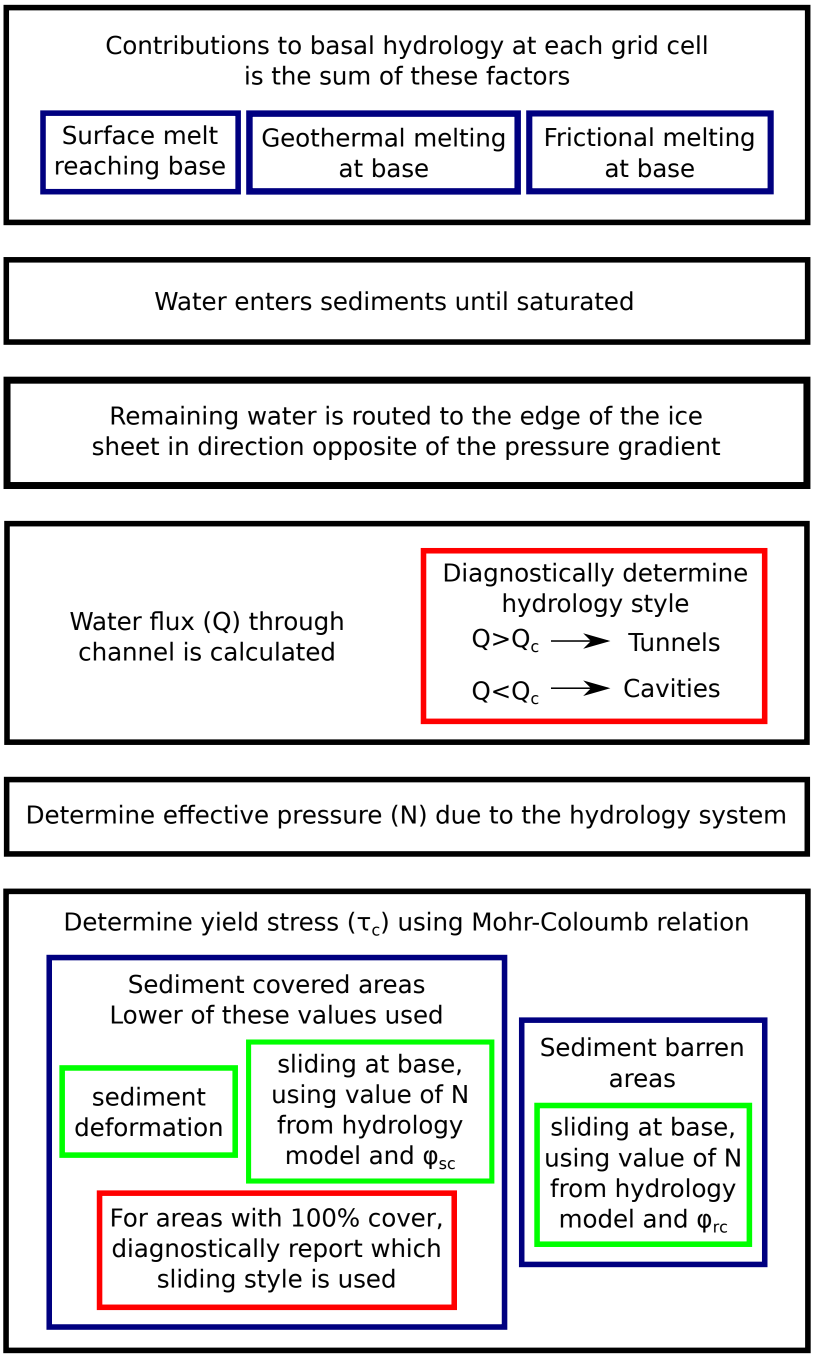

Fig. 2. Diagram showing the workflow of the model.

We use a simple subglacial water routing routine, where the water is transported in the direction opposite of the hydrological potential gradient, $\nabla\phi_h$. The equation for calculating the gradient at the base of the ice sheet is as in Cuffey and Paterson (2010):

$$-\nabla\phi_h = -\rho_i g \left[f_w \nabla S + \left[\frac{\rho_w}{\rho_i} - f_w \right] \nabla B \right] \tag{1}$$

In this equation, ρ_i is the ice density, ρ_w is the water density, g is the gravitational acceleration, ∇S is the ice surface gradient, ∇B is the bed gradient, and f_w is the "flotation fraction", which is the ratio of the water pressure and overburden pressure. The flotation fraction governs the relative influence of the bed and ice surface slopes on the direction of water flow. We have set it to be a constant, $f_w = 0.8$, which gives the surface slope a 2.7 times greater influence on the routing (Cuffey and Paterson, 2010). This ensures that the water will generally move towards the edge of the ice sheet. We calculate the gradient either using a third order finite difference method described in Skidmore (1989) or using a least squares method on a 5×5 grid, the later which is the default.

Although PISM generally works efficiently by breaking up the computation domain, the routing of water is most efficiently done on a single processor. However, we do utilize the efficiency of multiple processors to first sort the gradient, using a merge sort algorithm. To distribute the water, we first find the magnitude of the gradient, and set any grid cell below a threshold ice thickness to be zero. We then sort the grid cells from lowest to highest gradient on each processor into permutation arrays. For efficiency, the permutation arrays are stored as a variable since they are unlikely to change substantially between time steps. The sorted arrays are transfered to a single processor for the merge sort. The water flux within each sorted cell, T_w, is added to adjacent cells if the gradient is above a certain threshold (which we have set to be 1.0). The purpose of this threshold is to avoid singularities within the ice sheet, so any cell that has a gradient less than the threshold is set to have no water flux.

Effective pressure

To calculate the effective pressure, we use a parameterization described by Schoof (2010). This parameterization is based on the concept of water drainage at the bottom of the ice sheet being routed through efficient Röthlisberger channels (Röthlisberger, 1972) or less efficient linked cavities (Kamb, 1987). This is a modification of other subglacial drainage models that have been proposed in the past (Fowler, 1987; Hewitt and Fowler, 2008), but allows for better switching between drainage styles. The style of drainage system is dependent on the amount of water available and the velocity of the ice. In this formulation, the effective pressure decreases up to a certain point, after which drainage becomes efficient enough that it causes the effective pressure to increase again.

The main component of this model is the switch between channel and cavity drainage systems. The type of drainage system is dependent on the total water flux, Q. The threshold water flux, Q_c is calculated by the following equation:

$$Q_c = \frac{u_b k}{c_1(\alpha - 1)\nabla\phi_h} \tag{2}$$

The velocity of the ice at the base is u_b. In this model, the bed is assumed to have a roughness, with a protrusion height of k, which we have set to be 0.1 m. The constant c_1 is related to the latent heat of fusion of ice, L, and is calculated by $c_1 = 1/(\rho_i L)$. The constant $\alpha = 5/4$ is related to the Darcy–Weisbach law friction factor for water flow in a conduit (Schoof, 2010).

The water is assumed to be directed through a single channel. The total flux of water through a channel, Q, considering a grid cell of width dx is calculated as follows:

$$Q = \frac{T_w dx^2}{dx/r} \tag{3}$$

The value of r is the spacing between channels. For this value, we have set it to be a constant of 12 km, which is the average distance between eskers on the Canadian Shield (Storrar and others, 2014). This formulation allows for the proper parameterization of water flux through the channel regardless of the actual width of the grid cell. Based on Eq. 2, if $Q > Q_c$, then the routing is via the tunnel system (efficient drainage), while if $Q < Q_c$, the drainage is via an the cavity system (inefficient drainage). As a result of this formulation, if the ice velocity increases, the threshold amount of water to switch to efficient tunnel drainage also increases.

The effective pressure, N is calculated by the following equation (Schoof, 2010):

$$N^n = \frac{c_1 Q \nabla\phi_h + u_b h}{c_2 {c_3}^{-1/\alpha} Q^{1/\alpha} {\nabla\phi_h}^{-1/(2\alpha)}} \tag{4}$$

The exponent, n is the Glen exponent, which by default is 3. The thickness of the ice is h. The velocity of the ice at the base is u_b. The constant $c_2 = 2An^{-n}$ includes parameters in Glen's law, where A is the ice softness. The default value is $A = 3.1689 \times 10^{24}$ Pa^{-3} s^{-1} (Huybrechts and Payne, 1996). The constant c_3 is related to the relation for turbulent flow of water in the Darcy–Weisbach law, where $c_3 = 2^{1/4}\sqrt{\pi + 2}/[\pi^{1/4}\sqrt{\rho_w f}]$, and f is a friction factor. We use the value $f = 0.1$ (Schoof, 2010).

There is a check so that the calculated effective pressure is not greater than the overburden pressure:

$$N \leq \rho_i g h \tag{5}$$

If the effective pressure is greater than the threshold, it is set to be equal to the overburden pressure. There is also a check to ensure that the effective pressure is greater than a minimum threshold, which we have set to be 0.01 times the overburden pressure. In reality, this should rarely happen (*i.e.* if the equation was solved where there is essentially no ice, or where there is no surface gradient and velocity), and is only to ensure the stability of the ice sheet model.

Basal sliding model

The sliding model that we use is basically an expansion of the existing Mohr-Coloumb yield stress relationship that is generally used as the sliding law in PISM (Bueler and van Pelt, 2015). The modified sliding law has two components, sliding due to the deformation of saturated sediments, and sliding due to the interactions between the water in the drainage system and the ice-bed interface.

The Mohr-Coloumb yield stress, τ_c, is a function of the effective pressure, the angle of internal friction, ϕ, and a cohesion parameter, c.

$$\tau_c = N \tan(\phi) + c \tag{6}$$

The value of ϕ determines the angle that the material will fail (slip) if a normal stress is applied. In the default PISM sliding law, the entire base of the ice sheet is assumed to be covered in a layer of deformable sediments (*i.e* soft bedded sliding), and ϕ is the shear friction angle of the sediments. For sediments, this value will depend on the dominant grain size, with clay materials having a lower value than sand and gravel. When a sediment under the ice sheet becomes water saturated, the effective pressure decreases, which increases the chance of failure. In general, the cohesion is regarded as being negligible in a deforming till (Cuffey and Paterson, 2010), so it is set to $c = 0$.

Our modified sliding law allows for spatially variable sediment cover, as places such as the Canadian Shield in North America did not have complete sediment cover (*i.e* hard bedded sliding) (Fulton, 1995). This sliding law still allows for sediment deformation as utilized in the default PISM sliding law, and for slip at the ice-bed interface. In this sliding law, the strength of the bed is calculated for both sediment deformation and slip along the bed-ice interface, and the lower value is taken.

The fraction of the area that is covered in sediment, S_f is a variable that can be read in, to allow for spatially variable cover. This affects both components of the basal sliding model. For areas that have incomplete sediment cover, sediment deformation only happens for the fraction of the surface that has sediment, while the rest of the area is set to have a yield stress that is equal to the overburden pressure:

$$\tau_c = S_f \tau_{sediment} + (1 - S_f)\rho_i g h \tag{7}$$

Where $\tau_{sediment} = N \tan(\phi_{sediment})$ is the yield stress of the sediments. The result of this is that areas with incomplete sediment cover will be less likely to be influenced by sediment deformation as the primary mode of sliding. For clarity, in this manuscript we have denoted S_f as a percentage, but the input into PISM must be as a fraction.

For the second component of the sliding law with sliding along the base, the Mohr-Coulomb relationship is also used. In this case the ϕ value is related to the roughness of the interface between the ice and the bed (Iken, 1981; Cuffey and Paterson, 2010). A Coulomb-style law has been found to be sufficient to describe hard bedded sliding (Helanow and others, 2021). In this model, the base of the ice sheet is covered by bumps, with an upslope angle that is equal to ϕ. There is a separate value for sediment covered areas (ϕ_{sc}) and areas where the bed is rock (ϕ_{rc}), as it is assumed that sediment covered areas will be smoother.

$$\tau_c = S_f N \tan(\phi_{sc}) + (1 - S_f) N \tan(\phi_{rc}) \tag{8}$$

In our model, if the bed is covered in sediment, it is assumed that the value of ϕ will be less than if the bed is rock, since the ice will effectively smooth the base though erosion or accumulation. The values of ϕ for sediment covered and bare areas can be set by the user. The effective pressure is taken from the hydrology submodel described in the previous section.

After the yield stress for both sediment deformation and sliding at the base has been calculated, the lower of the two values is taken as the yield stress for calculating sliding. As a result, if sediment cover is almost complete, the effective yield stress will be similar to the default sliding law of PISM. We will discuss this more in the following section.

Limitations

In reality, if there was enough water under the ice sheet, it would cause the ice sheet to float (*i.e.* the water pressure would exceed the overburden pressure and N would be negative). The model does not take into account this possibility, and as a result limits the seasonal acceleration of the ice sheet. Another issue is the lack of water storage underneath the ice sheet. When the hydrological gradient reaches a localized low point within the ice sheet, the model currently is not set up to conserve this water. If enough water were to collect at such a point, it is likely that a subglacial lake would form. A future addition to this model that would make it more realistic would be to incorporate water conservation between time steps. This could be used to determine if a subglacial lake would form. The consequence of these limitations is that the modelled velocity of the ice sheet will be slower than reality.

MODELLING

Model setup

Most of the model parameters used in this study are the same as described in Niu and others (2019b), which we will briefly summarize here. For the stress balance of the ice sheet, we use a combination of the shallow ice (SIA) and shallow shelf (SSA) approximations. The SIA is solved in areas with low velocity, while the SSA component is used as a "sliding" law in PISM in areas where the velocity is high (Bueler and Brown, 2009). The surface mass balance is driven by the positive degree day method (Reeh, 1991). The precipitation and temperature fields are varied between two climate states using an index, as implemented by Niu and others (2019b). Marine-ice sheet interactions make use of the PISM-PIK parameterizations, which control the ice sheet behavior of ice shelves and the grounding line (Winkelmann and others, 2011; Albrecht and others, 2011; Levermann and others, 2012). Water in sediments decays at a rate of 1 mm/yr. The main changes to the setup described by Niu and others (2019b) are below.

For calving of floating ice shelves, we have modified the thickness calving scheme in PISM. The default version of this is that any floating ice less than 200 m would be calved. This might be appropriate for Antarctica, but in the shallow Hudson Bay, where tidal and wave driven stresses would be far less, this is not appropriate. In our initial experiments, this harsh calving criteria prevented the advance of the ice sheet into Hudson Bay. Our modified version changes the thickness criteria to be dependent on the water depth:

$$h_{min} < h = cb < h_{max} \tag{9}$$

In this equation, h_{min} is a minimum thickness of the ice shelf, h_{max} is the maximum thickness, b is the water depth, and c is a scaling parameter. For our experiments, we use $h_{max} = 200$, $c = 0.1$ and $h_{min} = 40$. Using this set of parameters, for $b < 2000$ m, the maximum thickness at the ice front is less than the 200 m value in the default thickness calving routine.

As we wish to test the impact of changing basal conditions in the context of terrestrially terminating ice sheets (as the southern and western margins of the Laurentide Ice Sheet were), we have chosen to use the purely elastic glacial isostatic adjustment (GIA) module in PISM. The Lingle-Clark model (Lingle and Clark, 1985; Bueler and others, 2007) with a viscous half-space mantle that was used in Niu and others (2019b) has a tendency to produce unrealistically depressed basins when applied to the glaciation of the Laurentide Ice Sheet, likely the result of the lack of a contrasting high viscosity lower mantle. These basins are often below sea level, which PISM interprets as being ocean basins. This is not desirable in our experiments, and the elastic deformation model allows us to avoid this problem. In addition, we have kept sea level as a constant to avoid sea level induced fluctuations of the ice sheet (*i.e.* Gomez and others, 2020).

Idealized circular ice sheet experiments

Overview

In order to test the effects of our basal conditions model, we have created an idealized setup that produces a circular ice sheet in the absence of differing basal conditions. We use a sinusoidal index with a period of 40 000 years, so that the coldest conditions happen at 20 000 years. As noted by Niu and others (2019a), the maximum size of the ice sheets in this kind of experiment happens after the minimum in coldness, in our case at about 25 000 years. This is a time that we chose to compare the results of the experiments, since the ice sheet was near the maximum growth, and the elevation differences at the edge of the ice sheet are not substantial between the experiments. At this point, the equilibrium line for melt and accumulation is increasing, which causes meltwater to be produced at the surface. After 25 000 years, there tends to be a rapid retreat of the ice sheet, because of the differing basal conditions. Fig. 3 shows the general setup for the experiments, including the ice surface elevation and ice thickness near the edge of the ice sheet. Since there are changes in the basal conditions, this results in differing ice thickness evolution.

Fig. 4 shows an example demonstrating the switching between different hydrology types and sliding mechanisms for one of the idealized experiments (plots for all of the experiments can be found in the Supplementary Material). This particular experiment shows that there is a switch from an inefficient cavity system to an efficient tunnel system as the volume water flux increases. In the case with 50% sediment cover, there is an initial increase in velocity at the start of the melt season, and a reduction once the more efficient drainage style is achieved. Though the cavity system is reestablished at the end of the melt season, there is not a corresponding restoration of high velocity, likely due to the dependence on velocity for calculating the effective pressure (Eq. 4). Once the melt season is over, the velocity goes to zero in areas

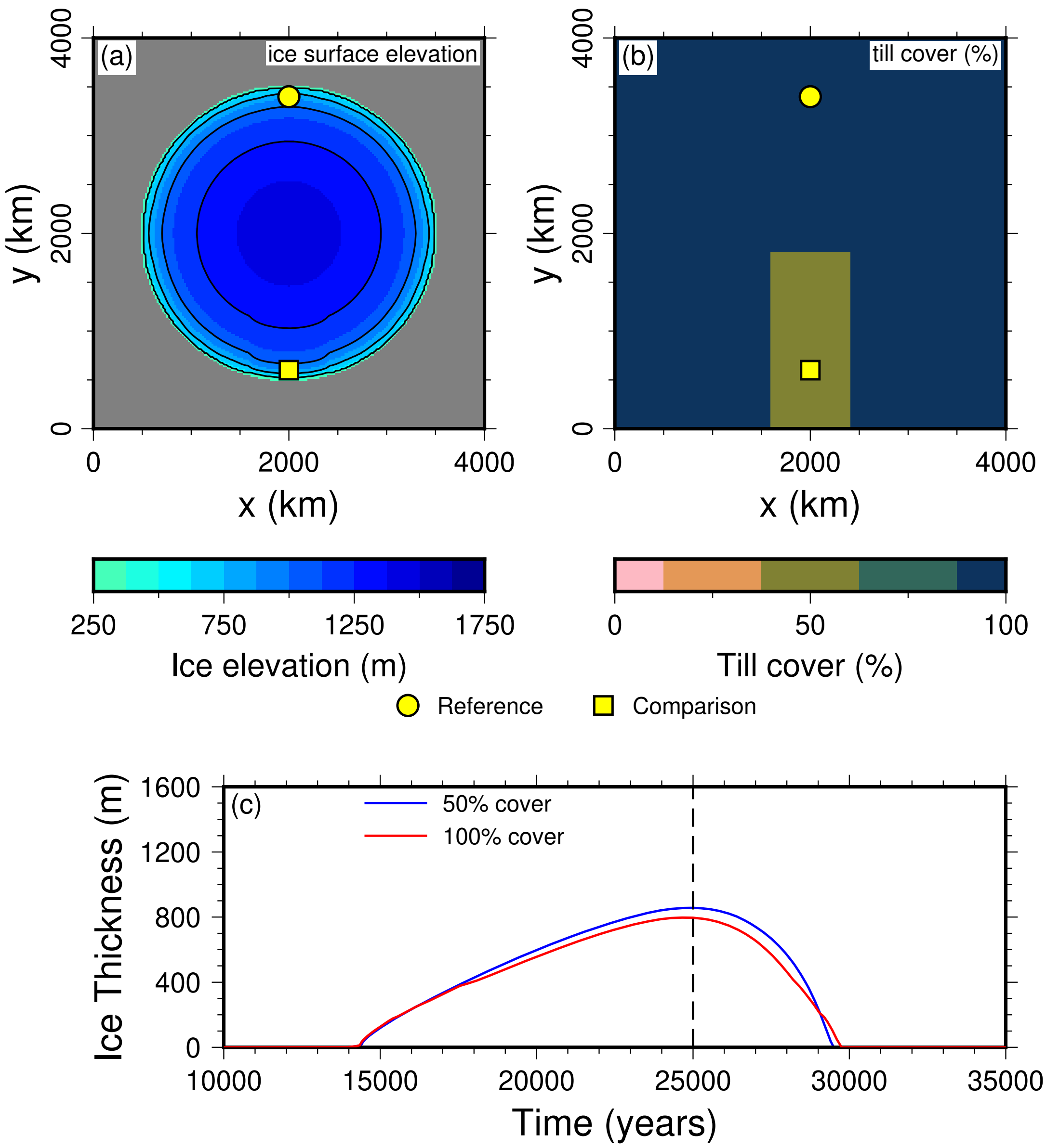

Fig. 3. Experiment with a strip of 50% sediment cover, with $\phi_{rc} = 2°$ for areas with bare rock, and $\phi_{sc} = 1$ for areas covered in sediment. The shear friction angle for sediment deformation is $\phi = 20°$. The percentage of surface meltwater reaching the base is 50%. (a) Ice surface elevation at 25 000 years. (b) Sediment (till) cover fraction, showing the strip with reduced cover. Also shown are the locations that are used to compare the velocity and sliding properties. (c) Ice thickness evolution at those two locations, showing that the thickness increases in the partially covered strip, as the velocity is less.

with incomplete sediment cover. For areas with sediment cover, velocity remains relatively high through the year due to the presence of deformable sediments, which decreases through the winter as the sediments slowly drain. During times of high discharge, the sliding mechanism switches from sediment deformation to sliding along the base, providing a spike in velocity during the summer.

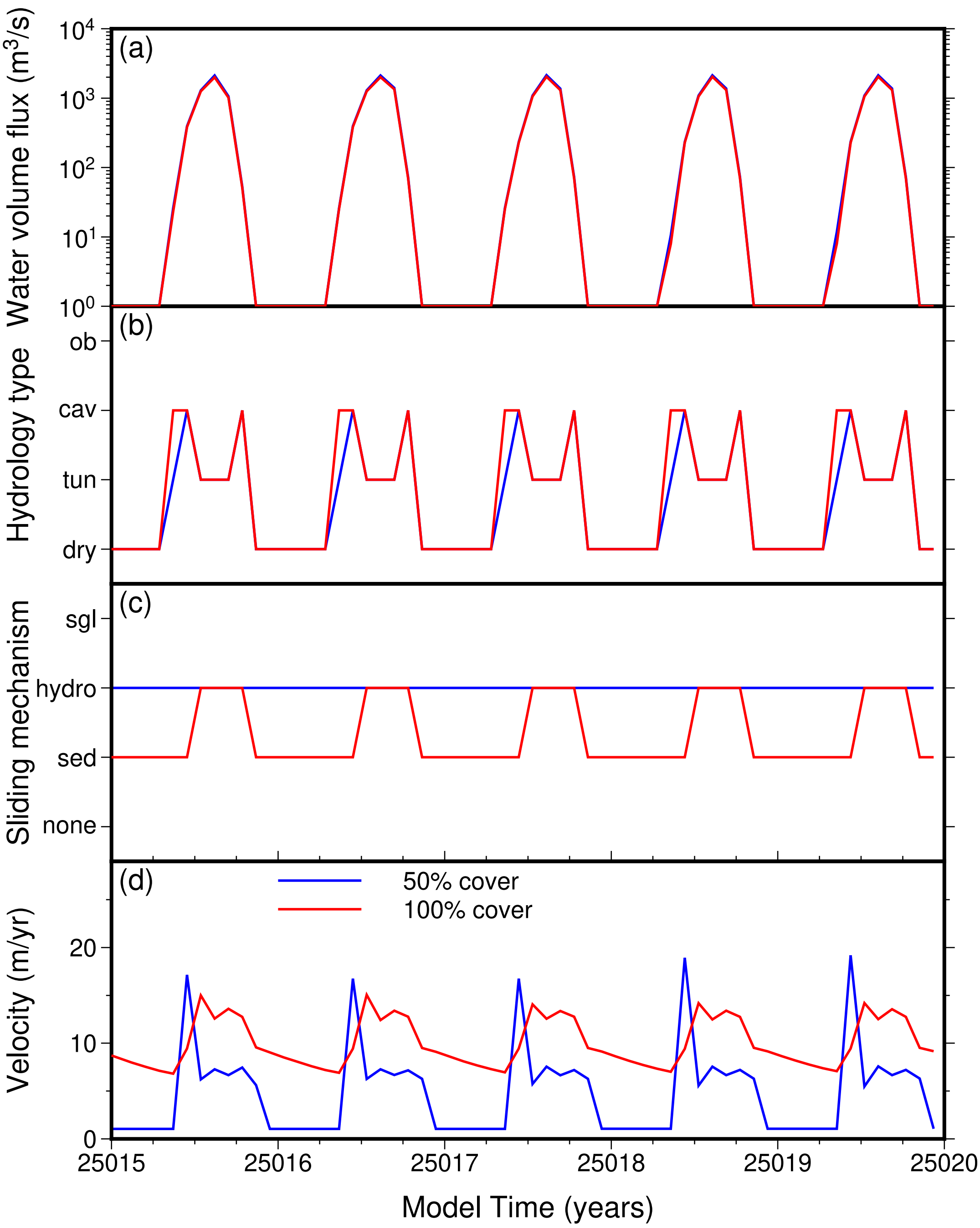

Fig. 4. Basal conditions and velocity time series for the locations shown in Fig. 3 at about 25 000 years. (a) Volume water flux, primarily from meltwater from the surface being transfered to the base. (b) Type of water routing at the base of the ice sheet that determines the effective pressure. ob - overburden, cav - cavities, tun - tunnels/channels, dry - no water in the system. (c) Sliding law method used by PISM. sgl - slippery grounding lines, hydro - modified sliding law that takes into account both sediment deformation and sliding at the ice-bed interface, sed - sediment deformation only model (PISM default), none - no sliding (*i.e.* purely overburden pressure). (d) Surface velocity magnitude at the location with 50% cover (blue) and 100% cover (red).

Effect of fraction sediment cover

We conducted a series of experiments where we set the strip of reduced sediment cover to be 50%, 80%, 95% and 99%. The purpose of this experiment is to see if there is a threshold where sediment deformation becomes important in partially covered regions. In these experiments, $\phi_{sediment} = 30°$ for sediment deformation, $\phi_{rc} = 15°$ for areas with bare rock, and $\phi_{sc} = 5°$ for areas covered in sediment. The amount of water reaching the base from the surface is 5%. In places with 100% sediment cover, sliding is always accomplished through sediment deformation, as the value of $\phi_{sc} = 5°$ seems too high to allow for sliding at the base. There is a slight increase in velocity during the summer, as the sediments become replenished and water saturated. For 50% and 80% cover, the velocity remains close to zero, as the sediment deformation is unable to overcome the resistance from bare regions. For 95% and 99% cover, the sliding velocity becomes comparable to the purely sediment covered ares, but drops a lot more when the supply of water is extinguished.

Effect of ϕ_{rc} and ϕ_{sc}

The initial default values of ϕ_{rc} and ϕ_{sc} were high, so it almost entirely prevented sliding except for sediment deformation. We tested a variety of values for ϕ_{rc} and ϕ_{sc} using both 50% and 95% sediment cover. For areas with 100% sediment cover, a switch to pure slip along the base did not happen unless $\phi_{sc} \leq 1°$. For areas with incomplete cover, decreasing $\phi_{rc} = 2°$ allowed sliding, while values above that prevented it. Using really low values ($\phi < 1°$) causes a great increase in velocity when water gets into the system, which can reach over 100 m/yr. Using such a small angle causes the ice sheet model to run very slowly, so this is not recommended for long duration runs.

Effect of $\phi_{sediment}$

We did many of the experiments with $\phi_{sediment} = 30°$ and $\phi_{sediment} = 20°$. With the higher value of $\phi_{sediment}$, the maximum velocity is generally less. During the melt season, the maximum velocity in the partially sediment cover areas increase a lot more when $\phi_{sediment}$ is lower. When ϕ_{rc} and ϕ_{sc} are set to lower values, the lower value of $\phi_{sediment}$ prevents the switch to the base sliding regime likely due to the higher initial velocity. This actually causes the maximum velocity in the $\phi_{sediment} = 30°$ experiments to be higher during the melt season, even though the annual average is lower.

Effect of water input

We tested different values of the fraction of surface meltwater reaching the base, using values of 0%, 0.05%, 20%, 50%, and 80%. Using 0% (which would be equivalent to the default in PISM), there is no sliding because there is essentially no water getting into the system, preventing the sediments from filling with water and deforming. When the fraction is higher than 20%, the switch from cavity to tunnel drainage styles is more likely to happen. In areas with complete sediment cover, the period of the melt season when the basal sliding happens instead of sediment deformation happens is also longer. There is only minimal difference between the 50% and 80% simulations, indicating there is an upper limit to how much the water input will affect the velocity after switching to the tunnel drainage system.

Evolution through the year

Generally, during the start of the melt season, there is a large spike in velocity, especially in regions that are not completely covered in sediment. As the amount of water increases, there is a switch from cavity to tunnel drainage styles, and there is a corresponding decrease in velocity. Later in the melt season when the water input decreases, the cavity system returns, but the corresponding jump in velocity is not as great, likely because the higher velocity causes the effective pressure to be higher. In areas that are completely sediment covered, the switch between sediment deformation to sliding on the base can also cause an increase in velocity during the melt season, though it is not always as large of a jump as in the incompletely covered areas. When the water input ends in the winter, the incompletely covered areas tend to have a velocity that is close to zero, while completely covered areas continue to have sliding. The velocity decreases through the winter as the water in the sediment slowly drains over time.

Glacial cycle simulation

In order to show the effect of different basal conditions on ice sheet evolution, we have repeated the experiment done by Niu and others (2019b) for the region covered by the Laurentide and Cordillera ice sheets in North America. The simulation runs for the past 120 000 years, using an index based on the NGRIP δ^{18} record (Andersen and others, 2004), with the value for full glacial conditions (1) corresponding to the Last Glacial Maximum (LGM) value at 21 000 yr BP, and a value of 0 to represent interglacial conditions at 0 yr BP. The climate forcing is from equilibrium simulations using the PMIP3 protocol from the COSMOS-AWI model (Stepanek and Lohmann, 2012; Zhang and others, 2013). We have edited the forcing to have zero precipitation outside of the Laurentide-Cordillera region to prevent ice sheet growth.

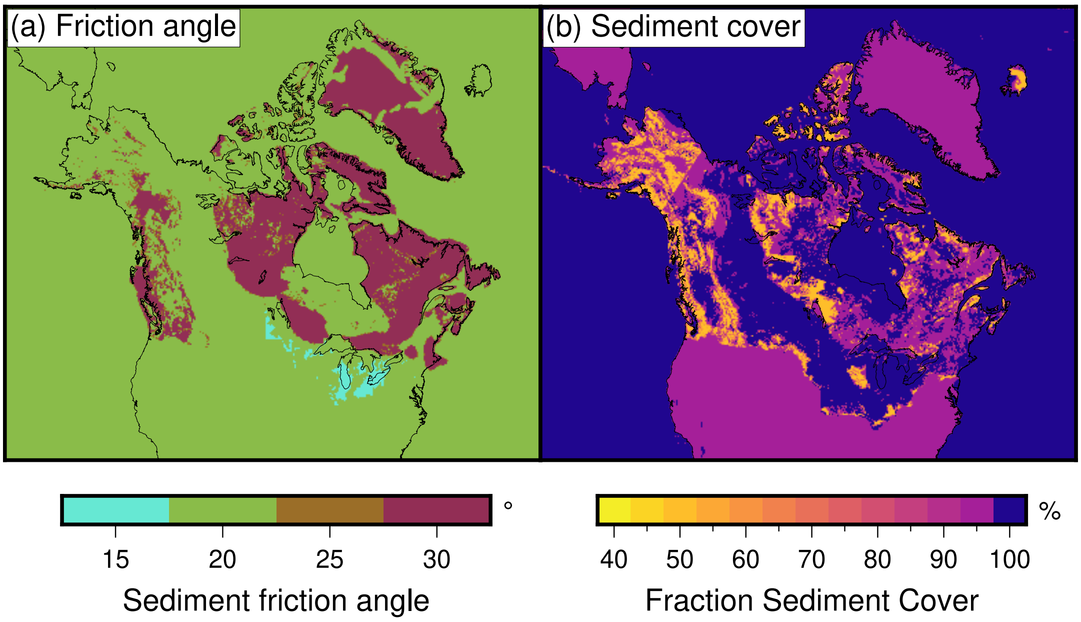

Fig. 5. Sediment properties used in the experiment (Gowan and others, 2019). (a) Sediment friction angle, used to govern the strength of the sediments. (b) Sediment cover distribution, showing areas of complete and incomplete sediment cover.

We compare the evolution of the ice sheet through the glacial cycle using two simulations. The default simulation (denoted "default") has the default "null" hydrology model used in PISM, where water is only created at the base through geothermal and frictional heating, and basal strength is defined through sediment deformation only (Tulaczyk and others, 2000). The second simulation (denoted "basal") has our new model as described earlier. In the basal simulation, we use $\phi_{rc} = 2°$, $\phi_{sc} = 1°$, and the fraction of surface meltwater reaching the base set to 50%.

The sediment properties for North America are derived from the dataset by Gowan and others (2019) (Fig. 5). In this dataset, there is parameterization for sediment grain size, and a generalized sediment cover distribution. For the sediment friction angle, we have set $\phi_{sediment} = 30°$ for sand, $\phi_{sediment} = 20°$ for silt, and $\phi_{sediment} = 15°$ for clay. These values are used for both experiments. For sediment cover, the fraction of the surface covered is set to 100% for "blanket" (*i.e.* complete cover), 95% for "veneer" (*i.e.* isolated bedrock outcrops), and 50% for "rock" (*i.e.* widespread bedrock outcrops). This is only applicable to the basal simulation.

The results of these simulations show that while the overall volume of both simulations is similar, the distribution of where the ice is can be quite different (Fig. 6). In the basal simulation, the ice advances faster, which allows more rapid buildup especially in areas with complete sediment cover. This results in places like Hudson Bay becoming fully covered in ice earlier in the simulation (Fig. 7). In the Last Glacial Maximum (20000 yr BP) time slice shown on Fig. 6, this is manifest in having thicker ice in western Laurentide region in the basal simulation. The default simulation has thicker ice in the core ice growth centers, which results in an overall greater ice volume. The basal simulation prevents the buildup of ice, and the volume stays stable through the LGM period. The absolute difference in ice volume between the simulations reaches up to 8 m of sea level equivalent (SLE, *i.e.* the equivalent water volume of ice divided by the area of the modern ocean).

DISCUSSION

Basal conditions model

The addition of a more realistic basal condition model impacts the maximum thickness of the ice sheet, and how quickly the ice can advance into areas with complete sediment cover. The main impact of our model comes from the inclusion of meltwater coming from the surface of the ice sheet, which allows sediments to saturate with water at a much faster rate. The secondary impact is that there is a larger contrast in dynamics between soft bedded areas with complete sediment cover and hard bedded areas with bedrock outcrops. In the glacial cycle simulation, this results in a thinner ice sheet in the core areas of the ice sheet, but thicker ice in peripheral regions.

The basal conditions model is designed to have low enough complexity to run at glacial cycles. The overhead at fully glacial conditions is roughly double that of the default model. This increase in overhead is largely the result of having seasonally variable water input, which results in sometimes rapidly varying velocity through the year. The sacrifice in speed is balanced by a more realistic depiction of ice sheet dynamics. The speed is slower than a default PISM run, because we limit the maximum interval of the adaptive time stepping mechanism to one month in order to capture the seasonal changes in the climate forcing (the unconstrained time step can be larger than than).

Our model is the first open source implementation of an ice sheet basal conditions model that allows for switching between tunnel and linked cavity styles of drainage, and between soft-bedded sediment deformation and hard-bedded sliding. This allows for a more complex parameterization of sliding than the default PISM model, which is governed exclusively by sediment deformation (Bueler and van Pelt, 2015). The BICICLES model uses a basal conditions model that switches between Coulomb (sediment deformation) and power law (basal sliding) modes depending on the amount of transported water (Gandy

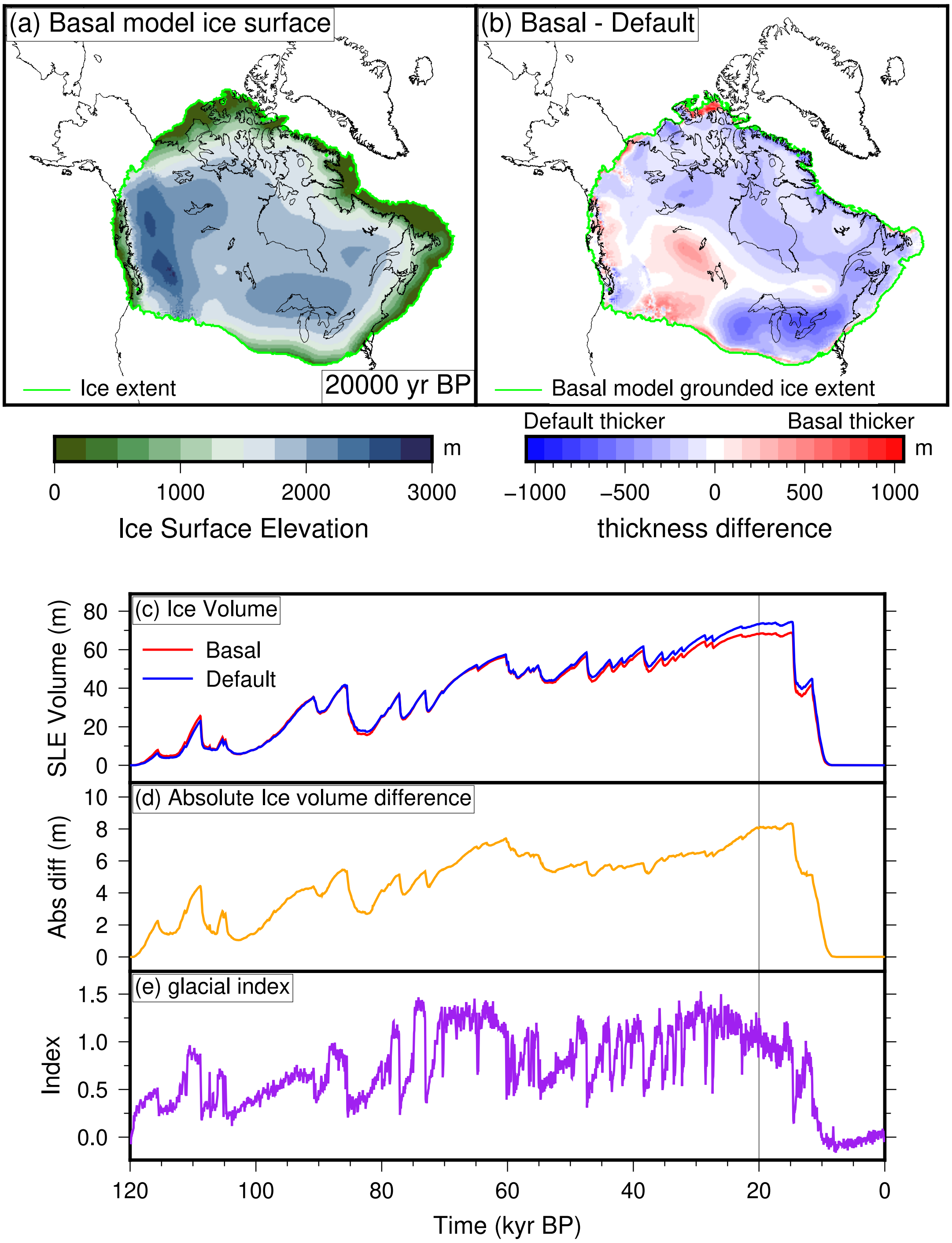

Fig. 6. Results of the glacial cycle simulation. (a) The ice surface elevation of the basal simulation at 20000 yr BP. (b) The absolute value of the difference between the basal and default grounded ice thickness at 20000 yr BP. (c) Ice volume evolution of the simulations. (d) Absolute ice volume difference between the simulations. (e) Glacial index used in the simulations, based on the Greenland ice core records (Andersen and others, 2004).

and others, 2019; Tsai and others, 2015), but does not have a mechanism for switching between drainage types. The CISM also allows for this kind of switching, but does not yet have basal water transport

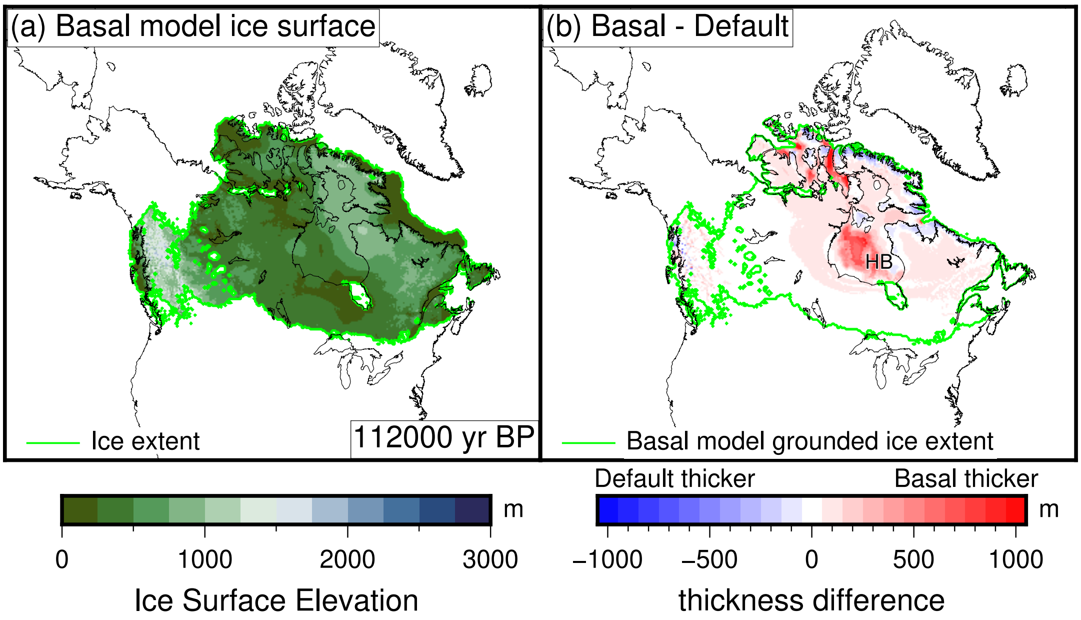

Fig. 7. Early ice advance into Hudson Bay (HB) in the basal simulation. (a) The ice surface elevation of the basal simulation at 112000 yr BP. (b) The absolute value of the difference between the basal and default grounded ice thickness.

(Lipscomb and others, 2019). SICOPOLIS includes the impact of variable basal hydrology on sliding (Clason and others, 2014; Gudlaugsson and others, 2017; Calov and others, 2018), but does not include the impact of sediment deformation. The switching to sediment deformation during winter allows for sliding to continue during low water input seasons, and we recommend implementing this style of basal sliding parameterization.

Implications for the Laurentide Ice Sheet evolution

Our new basal conditions model may provide a more realistic depiction of the initial growth of the Laurentide Ice Sheet. In Gowan and others (2021), it is hypothesized that the ice sheet initially advanced from the Labrador sector westward over Hudson Bay, something that is accomplished easier with our model. In the basal simulation, Hudson Bay becomes covered by the ice sheet much earlier, as the ice is able to flow fast enough to remain above the floating point, and therefore does not start calving. It was also hypothesized, based on non-glacial sediments possibly dated to MIS 3 located south of Hudson Bay (Dalton and others, 2019), that Hudson Bay may have been rapidly deglaciated and then quickly recovered. Our simulation was unable to simulate rapid deglaciation of Hudson Bay, possibly due to the lack of delayed GIA depression that was the likely driver (Abe-Ouchi and others, 2013; Bassis and others, 2017). Using our model shows that in an intermediate climate state it is possible for rapid advance to fill Hudson Bay through dynamic advance. The simulation also may show how the western areas of the Laurentide Ice Sheet became glaciated through dynamically advancing in the absence of a nearby precipitation source. The index based climate forcing that we use does not allow us to investigate this in detail, but as inferred in previous ice sheet modelling studies of the Laurentide Ice Sheet (*e.g.* Clark, 1994; Licciardi and others, 1998; Marshall and others, 2002; Gregoire and others, 2012; Stokes and others, 2012; Roberts and others, 2016; Wekerle and others, 2016), inclusion of spatially varying basal conditions are necessary to simulate the ice sheet.

CONCLUSIONS

We have presented a new basal conditions model for use in the ice sheet model PISM. This model allows us to incorporate spatially variable sediment parameters and basal hydrology that includes meltwater from the surface. Our model runs fast enough to be feasibly run for glacial cycles. The model, when applied to the Laurentide Ice Sheet, impacts how the ice sheet evolves, and changes the ultimate distribution and thickness of ice. Since the ice sheet is able to dynamically grow at a much faster rate, this provides a more realistic depiction of glacial advance. In future studies with a coupled climate forcing, we anticipate that our model will be better able to reproduce geological evidence of ice sheet extent and flow.

CODE AVAILABILITY

The version of PISM 1.0 with our basal conditions model can be found at `https://github.com/evangowan/pism_basal`. The scripts to generate the idealized circular ice sheet experiments can be found at `https://github.com/evangowan/pism_blackboard`.

ACKNOWLEDGEMENTS

This work was funded by the Helmholtz Climate Initiative REKLIM (Regional Climate Change), a joint research project of the Helmholtz Association of German research centres (HGF). This study was also supported by the Bundesministerium für Bildung und Forschung funded project PalMod, and the Program Changing Earth - Sustaining our Future of the Helmholtz Association. Development of PISM is supported by NSF grants PLR-1603799 and PLR-1644277 and NASA grant NNX17AG65G. The figures were created with the aid of Generic Mapping Tools (Wessel and others, 2019).

AUTHOR CONTRIBUTION STATEMENT

EJG came up with the concept for the basal conditions model, with input from CC and GL. EJG wrote the model code with contributions from SH. LN and SH developed the design of the PISM experiments, which were modified by EJG. EJG wrote the manuscript with input from all authors.

REFERENCES

Abe-Ouchi A and 6 others (2013) Insolation-driven 100,000-year glacial cycles and hysteresis of ice-sheet volume. *Nature*, **500**(7461), 190–193 (doi: 10.1038/nature12374)

Albrecht T, Martin M, Haseloff M, Winkelmann R and Levermann A (2011) Parameterization for subgrid-scale motion of ice-shelf calving fronts. *The Cryosphere*, **5**(1), 35–44 (doi: 10.5194/tc-5-35-2011)

Alley RB, Blankenship DD, Bentley CR and Rooney S (1986) Deformation of till beneath ice stream B, West Antarctica. *Nature*, **322**(6074), 57–59 (doi: 10.1038/322057a0)

Anandakrishnan S and Winberry JP (2004) Antarctic subglacial sedimentary layer thickness from receiver function analysis. *Global and Planetary Change*, **42**(1), 167 – 176, ISSN 0921-8181 (doi: 10.1016/j.gloplacha.2003.10.005), ice sheets and neotectonics

Andersen KK and 10 others (2004) High-resolution record of the Northern Hemisphere climate extending into the last interglacial period. *Nature*, **431**, 147–151 (doi: 10.1038/nature02805)

Arnold N and Sharp M (2002) Flow variability in the scandinavian ice sheet: modelling the coupling between ice sheet flow and hydrology. *Quaternary Science Reviews*, **21**(4), 485–502 (doi: 10.1016/S0277-3791(01)00059-2)

Aschwanden A, Bueler E, Khroulev C and Blatter H (2012) An enthalpy formulation for glaciers and ice sheets. *Journal of Glaciology*, **58**(209), 441–457 (doi: 10.3189/2012JoG11J088)

Bartholomew I, Nienow P, Sole A, Mair D, Cowton T and King MA (2012) Short-term variability in greenland ice sheet motion forced by time-varying meltwater drainage: Implications for the relationship between subglacial drainage system behavior and ice velocity. *Journal of Geophysical Research: Earth Surface*, **117**(F3), F03002 (doi: 10.1029/2011JF002220)

Bassis JN, Petersen SV and Mac Cathles L (2017) Heinrich events triggered by ocean forcing and modulated by isostatic adjustment. *Nature*, **542**(7641), 332–334 (doi: 10.1038/nature21069)

Bernales J, Rogozhina I, Greve R and Thomas M (2017) Comparison of hybrid schemes for the combination of shallow approximations in numerical simulations of the Antarctic Ice Sheet. *The Cryosphere*, **11**(1), 247–265 (doi: 10.5194/tc-11-247-2017)

Bueler E and Brown J (2009) Shallow shelf approximation as a “sliding law” in a thermodynamically-coupled ice sheet model. *Journal of Geophysical Research: Earth Surface*, **114**(F3), F03008 (doi: 10.1029/2008JF001179)

Bueler E and van Pelt W (2015) Mass-conserving subglacial hydrology in the parallel ice sheet model version 0.6. *Geoscientific Model Development*, **8**(6), 1613–1635 (doi: 10.5194/gmd-8-1613-2015)

Bueler E, Lingle CS and Brown J (2007) Fast computation of a viscoelastic deformable earth model for ice-sheet simulations. *Annals of Glaciology*, **46**, 97–105 (doi: 10.3189/172756407782871567)

Calov R and Greve R (2005) A semi-analytical solution for the positive degree-day model with stochastic temperature variations. *Journal of Glaciology*, **51**(172), 173–175 (doi: 10.3189/172756505781829601)

Calov R and 8 others (2018) Simulation of the future sea level contribution of Greenland with a new glacial system model. *The Cryosphere*, **12**(10), 3097–3121 (doi: 10.5194/tc-12-3097-2018)

Clark PU (1994) Unstable behavior of the Laurentide Ice Sheet over deforming sediment and its implications for climate change. *Quaternary Research*, **41**(1), 19–25 (doi: 10.1006/qres.1994.1002)

Clason C, Applegate P and Holmlund P (2014) Modelling Late Weichselian evolution of the Eurasian ice sheets forced by surface meltwater-enhanced basal sliding. *Journal of Glaciology*, **60**(219), 29–40 (doi: 10.3189/2014JoG13J037)

Clason CC and 6 others (2015) Modelling the transfer of supraglacial meltwater to the bed of leverett glacier, southwest greenland. *The Cryosphere*, **9**(1), 123–138 (doi: 10.5194/tc-9-123-2015)

Cornford SL and 8 others (2013) Adaptive mesh, finite volume modeling of marine ice sheets. *Journal of Computational Physics*, **232**(1), 529–549 (doi: 10.1016/j.jcp.2012.08.037)

Cuffey KM and Paterson WSB (2010) *The physics of glaciers*. Elsevier, Burlington, MA, USA

Dalton AS, Finkelstein SA, Forman SL, Barnett PJ, Pico T and Mitrovica JX (2019) Was the Laurentide Ice Sheet significantly reduced during marine isotope stage 3? *Geology*, **47**(2), 111–114 (doi: 10.1130/G45335.1)

Fowler AC (1987) Sliding with cavity formation. *Journal of Glaciology*, **33**(115), 255–267 (doi: 10.3198/1987JoG33-115-255-267)

Fulton RJ (1995) Surficial materials of Canada. Map 1880A, Geological Survey of Canada (doi: 10.4095/205040), scale 1:5 000 000

Gagliardini O, Cohen D, Råback P and Zwinger T (2007) Finite-element modeling of subglacial cavities and related friction law. *Journal of Geophysical Research: Earth Surface*, **112**(F2), F02027 (doi: 10.1029/2006JF000576)

Gandy N, Gregoire LJ, Ely JC, Cornford SL, Clark CD and Hodgson DM (2019) Exploring the ingredients required to successfully model the placement, generation, and evolution of ice streams in the British-Irish Ice Sheet. *Quaternary Science Reviews*, **223**, 105915 (doi: 10.1016/j.quascirev.2019.105915)

Gomez N, Weber ME, Clark PU, Mitrovica JX and Han HK (2020) Antarctic ice dynamics amplified by Northern Hemisphere sea-level forcing. *Nature*, **587**(7835), 600–604 (doi: 10.1038/s41586-020-2916-2)

Gowan EJ, Niu L, Knorr G and Lohmann G (2019) Geology datasets in North America, Greenland and surrounding areas for use with ice sheet models. *Earth System Science Data*, **11**(1), 375–391 (doi: 10.5194/essd-11-375-2019)

Gowan EJ and 9 others (2021) A new global ice sheet reconstruction for the past 80 000 years. *Nature Communications*, **12**, 1199 (doi: 10.1038/s41467-021-21469-w)

Greenwood SL, Clason CC, Nyberg J, Jakobsson M and Holmlund P (2017) The Bothnian Sea ice stream: early Holocene retreat dynamics of the south-central Fennoscandian Ice Sheet. *Boreas*, **46**(2), 346–362 (doi: https://doi.org/10.1111/bor.12217)

Gregoire LJ, Payne AJ and Valdes PJ (2012) Deglacial rapid sea level rises caused by ice-sheet saddle collapses. *Nature*, **487**(7406), 219–222 (doi: 10.1038/nature11257)

Gudlaugsson E, Humbert A, Andreassen K, Clason CC, Kleiner T and Beyer S (2017) Eurasian ice-sheet dynamics and sensitivity to subglacial hydrology. *Journal of Glaciology*, **63**(239), 556–564 (doi: 10.1017/jog.2017.21)

Helanow C, Iverson NR, Woodard JB and Zoet LK (2021) A slip law for hard-bedded glaciers derived from observed bed topography. *Science Advances*, **7**(20) (doi: 10.1126/sciadv.abe7798)

Hewitt IJ and Fowler AC (2008) Seasonal waves on glaciers. *Hydrological Processes*, **22**(19), 3919–3930 (doi: 10.1002/hyp.7029)

Huybrechts P and Payne T (1996) The EISMINT benchmarks for testing ice-sheet models. *Annals of Glaciology*, **23**, 1–12 (doi: 10.3189/S0260305500013197)

Iken A (1981) The effect of the subglacial water pressure on the sliding velocity of a glacier in an idealized numerical model. *Journal of Glaciology*, **27**(97), 407–421 (doi: 10.3189/S0022143000011448)

Joughin I, MacAyeal DR and Tulaczyk S (2004) Basal shear stress of the Ross ice streams from control method inversions. *Journal of Geophysical Research*, **109**, B09405 (doi: 10.1029/2003JB002960)

Kamb B (1987) Glacier surge mechanism based on linked cavity configuration of the basal water conduit system. *Journal of Geophysical Research*, **92**(B9), 9083–9100 (doi: 10.1029/JB092iB09p09083)

Levermann A, Albrecht T, Winkelmann R, Martin MA, Haseloff M and Joughin I (2012) Kinematic first-order calving law implies potential for abrupt ice-shelf retreat. *The Cryosphere*, **6**(2), 273–286 (doi: 10.5194/tc-6-273-2012)

Licciardi J, Clark P, Jenson J and Macayeal D (1998) Deglaciation of a soft-bedded Laurentide Ice Sheet. *Quaternary Science Reviews*, **17**, 427–448 (doi: 10.1016/S0277-3791(97)00044-9)

Lingle CS and Clark JA (1985) A numerical model of interactions between a marine ice sheet and the solid earth: Application to a West Antarctic ice stream. *Journal of Geophysical Research: Oceans*, **90**(C1), 1100–1114 (doi: 10.1029/JC090iC01p01100)

Lipscomb WH and 14 others (2019) Description and evaluation of the Community Ice Sheet Model (CISM) v2.1. *Geoscientific Model Development*, **12**(1), 387–424 (doi: 10.5194/gmd-12-387-2019)

Margold M, Stokes CR and Clark CD (2015) Ice streams in the Laurentide Ice Sheet: Identification, characteristics and comparison to modern ice sheets. *Earth-Science Reviews*, **143**, 117–146

Marshall S, James T and Clarke G (2002) North American ice sheet reconstructions at the last glacial maximum. *Quaternary Science Reviews*, **21**(1-3), 175–192, ISSN 0277-3791 (doi: 10.1016/S0277-3791(01)00089-0)

Morlighem M, Rignot E, Seroussi H, Larour E, Ben Dhia H and Aubry D (2010) Spatial patterns of basal drag inferred using control methods from a full-Stokes and simpler models for Pine Island Glacier, West Antarctica. *Geophysical Research Letters*, **37**(14), L14502 (doi: 10.1029/2010GL043853)

Niu L, Lohmann G and Gowan EJ (2019a) Climate noise influences ice sheet mean state. *Geophysical Research Letters*, **46**(16), 9690–9699 (doi: 10.1029/2019GL083717)

Niu L, Lohmann G, Hinck S, Gowan EJ and Krebs-Kanzow U (2019b) The sensitivity of Northern Hemisphere ice sheets to atmospheric forcing during the last glacial cycle using PMIP3 models. *Journal of Glaciology*, **65**, 645–661 (doi: 10.1017/jog.2019.42)

PISM authors (2017) PISM, a Parallel Ice Sheet Model. Accessed October 19, 2017

Reeh N (1991) Parameterization of melt rate and surface temperature in the Greenland Ice Sheet. *Polarforschung*, **59**(3), 113–128 (doi: 10013/epic.29636.d001)

Roberts WHG, Payne AJ and Valdes PJ (2016) The role of basal hydrology in the surging of the Laurentide Ice Sheet. *Climate of the Past*, **12**(8), 1601–1617 (doi: 10.5194/cp-12-1601-2016)

Röthlisberger H (1972) Water pressure in intra- and subglacial channels. *Journal of Glaciology*, **11**(62), 177–203 (doi: 10.3189/S0022143000022188)

Schoof C (2010) Ice-sheet acceleration driven by melt supply variability. *Nature*, **468**(7325), 803–806

Shapero DR, Joughin IR, Poinar K, Morlighem M and Gillet-Chaulet F (2016) Basal resistance for three of the largest greenland outlet glaciers. *Journal of Geophysical Research: Earth Surface*, **121**, 168–180 (doi: 10.1002/2015JF003643)

Skidmore AK (1989) A comparison of techniques for calculating gradient and aspect from a gridded digital elevation model. *International Journal of Geographical Information Systems*, **3**(4), 323–334 (doi: 10.1080/02693798908941519)

Stepanek C and Lohmann G (2012) Modelling mid-Pliocene climate with COSMOS. *Geoscientific Model Development*, **5**(5), 1221–1243 (doi: 10.5194/gmd-5-1221-2012)

Stokes CR and Clark CD (2001) Palaeo-ice streams. *Quaternary Science Reviews*, **20**(13), 1437–1457, ISSN 0277-3791 (doi: 10.1016/S0277-3791(01)00003-8)

Stokes CR, Tarasov L and Dyke AS (2012) Dynamics of the North American Ice Sheet Complex during its inception and build-up to the Last Glacial Maximum. *Quaternary Science Reviews*, **50**, 86–104 (doi: 10.1016/j.quascirev.2012.07.009)

Storrar RD, Stokes CR and Evans DJ (2014) Morphometry and pattern of a large sample (> 20,000) of canadian eskers and implications for subglacial drainage beneath ice sheets. *Quaternary Science Reviews*, **105**, 1–25 (doi: 10.1016/j.quascirev.2014.09.013)

Tsai VC, Stewart AL and Thompson AF (2015) Marine ice-sheet profiles and stability under Coulomb basal conditions. *Journal of Glaciology*, **61**(226), 205–215 (doi: 10.3189/2015JoG14J221)

Tulaczyk S, Kamb WB and Engelhardt HF (2000) Basal mechanics of Ice Stream B, West Antarctica: 2. Undrained plastic bed model. *Journal of Geophysical Research: Solid Earth*, **105**(B1), 483–494 (doi: 10.1029/1999JB900328)

van de Wal RSW and 6 others (2008) Large and rapid melt-induced velocity changes in the ablation zone of the Greenland Ice Sheet. *Science*, **321**(5885), 111–113 (doi: 10.1126/science.1158540)

Walter F, Chaput J and Lüthi MP (2014) Thick sediments beneath Greenland's ablation zone and their potential role in future ice sheet dynamics. *Geology*, **42**(6), 487–490 (doi: 10.1130/G35492.1)

Wekerle C, Colleoni F, Näslund JO, Brandefelt J and Masina S (2016) Numerical reconstructions of the penultimate glacial maximum northern hemisphere ice sheets: sensitivity to climate forcing and model parameters. *Journal of Glaciology*, **62**(234), 607–622 (doi: 10.1017/jog.2016.45)

Wessel P and 6 others (2019) The Generic Mapping Tools Version 6. *Geochemistry, Geophysics, Geosystems*, **20**(11), 5556–5564 (doi: 10.1029/2019GC008515)

Winkelmann R and 6 others (2011) The Potsdam Parallel Ice Sheet Model (PISM-PIK) – Part 1: Model description. *The Cryosphere*, **5**(3), 715–726 (doi: 10.5194/tc-5-715-2011)

Zhang X, Lohmann G, Knorr G and Xu X (2013) Different ocean states and transient characteristics in Last Glacial Maximum simulations and implications for deglaciation. *Climate of the Past*, **9**(5), 2319–2333 (doi: 10.5194/cp-9-2319-2013)

Zwally HJ, Abdalati W, Herring T, Larson K, Saba J and Steffen K (2002) Surface melt-induced acceleration of Greenland ice-sheet flow. *Science*, **297**(5579), 218–222 (doi: 10.1126/science.1072708)

APPENDIX

Command line options

Table 1. Command line options available for the described models

Option	Default value	Description
-hydrology_fraction_from_surface	0.8	Fraction of the surface meltwater that is transfered to the base of the ice sheet
-ice_thickness_threshold	5.0	Ice thickness threshold under which water is not transported
-hydrology_tunnel_spacing	12000	Distance between Röthlisberger channels (in m)
-till_fraction_coverage	1.0	default fraction of surface covered in sediments
-floatation_fraction	0.8	ratio of the pressure of water to the pressure of ice, and will influence the effect of the bed gradient on the total potential gradient
-rocky_phi	15	value of ϕ for areas not covered by sediment
-seddy_phi	5	value of ϕ for areas covered by sediment